ISSN: 2634-9221
European Journal of Applied Sciences; Vol. 14 No. 05 (2026) (541-565)
https://doi.org/10.14738/ejas.1405.12526

New Insights into the Mathematical and Physical Treatment of the Flat Plate Boundary Layer Theory

Emerson Freitas Jaguaribe*

Departamento de Engenharia Mecânica - Centro de Tecnologia – Campus I da UFPB – 58051 900, João Pessoa – PB – Brazil

Abstract: A solution can effectively challenge the core principles of integral calculus, particularly when it comes to ordinary differential equations, as illustrated by Blasius's notable theory of the flat plate boundary layer. A third-order ordinary differential equation is solved using four boundary conditions. While this model is well known for illustrating various aspects of uniform flow over a flat plate, it is classically associated with another flow, supposedly easier to analyze and treat, produced by a towed plate in the same fluid at rest. This association stems from the mistaken belief that both flows are adjusted by changing their velocity reference frame. The classical solution method of the modified system of differential equations does not guarantee the uniqueness of the solution. It estimates the first nonzero term of the series solution as a constant and an unknown, while ignoring the Eulerian reference frame when addressing the continuity equation. A deeper analysis of the issue at hand has paved the way for developing a different model. This new approach acknowledges that the first nonzero term of the series solution is a function of viscosity. This understanding enables the derivation of both nondimensional velocity components that are consistent with Prandtl's boundary layer concepts. With these elements, it becomes easy to address local skin-friction effects and determine the exact vortex equation, thereby enabling exploration of the dynamic actions of both physical quantities in the boundary layer.

Keywords: Blasius´s solution of the flat plate boundary layer, New equations, Transition from laminar to turbulence, Environmental forcing, Vorticity.

INTRODUCTION

An in-depth analysis of the classic flat plate model proposed by Blasius [1] reveals significant mathematical errors and conflicting physical interpretations. A crucial finding commented on by Van Dyke [2] is that the model's solution is not unique. While many authors, such as Sissom and Pitts [3] regard this solution as "an outstanding early successful application of boundary layer theory" and Houghton et al. [4] suggest it is "a model to gain insight into the laminar boundary layer concept", there are underlying issues. Guran and Gwinner [5] raise a concern on page 335 about this solution: "The problem was first solved by Blasius using a series expansion method. However, the proposed analytic series solution does not converge at all."

Von Kármán's [6, 7] flat-plate integral method, known as the approximate method for analyzing the flat-plate boundary layer, presents similar difficulties, as explained by Jaguaribe [8]. According to Rohsenow and Choi [9], this alternative approximate integral method provides results only for the friction coefficient, whereas Blasius's "exact" solution yields both velocity distribution and friction coefficient. On the other hand, Pritchard and Michel [10] and Welty, Rorrer, and Foster [11] view it as a general expression, noting that

it applies equally well to turbulent boundary layers. Additionally, Welty et al. [12] believe it is a means of validating the flat-plate Reynolds analogy.

Although the scientific community has consistently acknowledged the error-free nature of Blasius's classical solution, grave faults are evident, as will be demonstrated first by outlining inconsistencies in the physical model and then by addressing flaws in the mathematical context.

Common Misconceptions

Concerning the Physical Model

The Neglected Eulerian Frame:

Figure 1 illustrates the main aspects of a typical laminar boundary layer, showing constant-property flow moving smoothly over a flat plate at a steady free stream velocity, denoted as U∞, at a zero-degree angle of incidence. In this context, the continuity equation is presented in its differential form, as shown in Equation (1).

$$\frac{\partial u}{\partial x}+\frac{\partial v}{\partial y}=0 \tag{1}$$

where u and v are, respectively, the x- and y-direction velocity components. The flow dynamics illustrated in Figure 1 clearly demonstrate how the physical structure influences the dynamic development of a viscous flow. Examining the various hydrodynamic consequences of a uniform flow crossing a control surface indicates that the most suitable representation of the continuity equation is its integral form. However, if we retain the continuity equation in its differential form, we can adjust the velocity components in the x and y directions accordingly:

$$u=\mathrm{U}_{\infty}\frac{\mathrm{df}}{\mathrm{d}\eta} \tag{2}$$

$$v=\frac{1}{2}\sqrt{\frac{\nu \mathrm{U}_{\infty}}{x}}\left(\eta\frac{\mathrm{df}}{\mathrm{d}\eta}-\mathrm{f}\right) \tag{3}$$

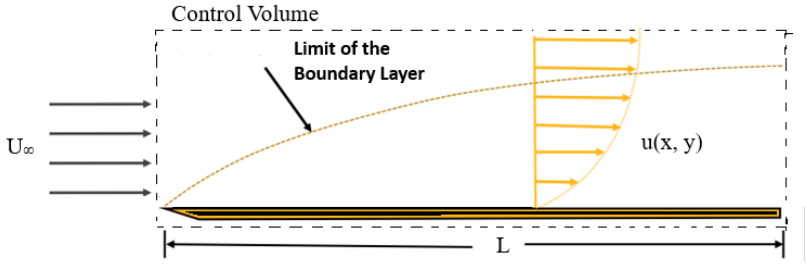


Figure 1: A typical sketch of a laminar boundary layer.

where ν is the kinematic viscosity, η is the similarity parameter, and f(η) is the dimensionless stream function; see Rohsenow and Choi [9], Sissom and Pitts [3], or Bennett and Myers [12]. The boundary conditions for solving the Blasius equation are:

$$\frac{\partial \mathrm{f}}{\partial\eta}\Big)_{\eta_{\infty}}=1, \tag{4}$$

$$\mathrm{f}(0)=0 \tag{5}$$

$$\frac{\partial f}{\partial \eta}\Big)_0 = 0 \tag{6}$$

As we know, the boundary layer outline separates the viscous flow from the potential flow; thus, $v(\eta_\infty)$ should be null. It is easy to see, considering Equations (3) and (4), that the potential flow occurs just for $f(\eta_\infty) = \eta_\infty$. However, if $v(\eta_\infty) = 0$, the resulting velocity distribution – refer to Equation (2) - leads to x-direction velocity component within the boundary layer exceeding the free stream velocity, U_∞, by more than 43%, as shown in Jaguaribe [13]. Therefore, this flow pattern is not realistic. On the other hand, if $v > 0$ it indicates that the flow moves through the boundary layer, thereby counteracting the fluid deceleration caused by viscosity. As a result, potential flow does not occur. Rohsenow and Choi [9] use Equation (3) on page 39 to describe the velocity component in the y-direction. They also provide the classic graph showing $v > 0$ at η_∞, along with an explanation of the physically unacceptable results as an anomaly. Although the pattern may seem unrealistic, the authors, along with Sissom and Pitts [3], highlight that Blasius's solution, as presented, aligns with classical boundary layer theory, without questioning the model's conception, solution, or results.

Why not apply the continuity equation in its differential form in the configuration under analysis? To study a moving fluid within the boundary layer, disturbances affecting laminar flow require an Eulerian reference frame to estimate various effects on the fluid. Selecting an appropriate control volume around the apparatus (the plate) is essential for evaluating the effect of inflow on the entire boundary layer. The continuity equation should ensure a mass balance that accurately represents the net mass entering and exiting the control volume within a representative section of the boundary layer, as shown in Figure 1. On the other hand, the differential form of the continuity equation is insensitive to inflow crossing the control-surface boundary at the leading edge. It ignores the velocity profile type, velocity magnitudes, direction, possible periodicity, and so on, which, as is obvious, are crucial to boundary-layer formation and behavior. Therefore, it is necessary to integrate the continuity equation over a finite element of the plate (Δx), bounded by the boundary layer, as shown in Jaguaribe [14, 15].

The Towed Plate and the Galilean Reference:

Discussing the momentum theorem, von Kármán [16, 17] stated, "The subsequent report by Pohlhausen [18] contains the calculations for several practically important cases, so that this method need not be gone into further." His calculations show that in all cases computed using Prandtl's partial differential equations, the approximate method yields results that are commensurate for all practical purposes. However, more singular is von Kármán's view concerning the laminar and turbulent boundary layer: "The simplest and practically most important case that the boundary layer theory deals with is the frictional resistance of a plate **towed** in a fluid at rest parallel to its plane." (author's bold type reference). However, upon examining this perspective in detail, we find that the mathematical solution to the problem of a towed plate moving at a free stream velocity in a still fluid presents, obviously, different boundary conditions from those involved in the mathematical resolution of the problem of uniform flow over a flat plate. Thus, we have two different mathematical solutions and two different results.

On the other hand, considering both physical resultant structures, we observe that the kinetic field of the potential flow developed by the towed plate is characterized by null velocities, which lie on a single line corresponding to the boundary layer edge. In contrast, the location of the one related to the uniform flow can be much broader due to the free stream velocity passing over the edge of the boundary layer. Comparing the two boundary layers, we conclude that they correspond to two different scenarios, which hampers analysis based solely on Galilean invariance.

Misinterpretation of the Velocity Gradient, du/dy, as y → ∞:

Some authors, such as Weinan [18], consider that a "problem in the mathematical analysis of fluid dynamics is the asymptotic limit of the fluid flow as viscosity goes to zero." However, as *y* approaches infinity, the gradient of the *u* component, specifically d*u*/d*y*, approaches zero. It is certainly necessary to consider in detail the underlying mechanism involving this process.

Concerning Mathematical Flaws

Utilizing an additionally artificial and non-conforming fourth boundary condition to solve a third-order nonlinear ordinary differential equation:

The Blasius equation:

$$\mathrm{f}(\eta)\frac{\partial^2 \mathrm{f}(\eta)}{\partial \eta^2} + 2\frac{\partial^3 \mathrm{f}(\eta)}{\partial \eta^3} = 0 \tag{7}$$

having the natural boundary conditions given by Equations (4) up to (6), is a third-order nonlinear ordinary differential equation, corresponding to a two-point boundary value problem, thus requiring just three boundary conditions to be solved.

Wu et al. [19] discuss the solution of Equation (7), mentioning the natural boundary conditions given by Equations (4) up to (6), and considering the classical series solution f(η). Then, they commented that f"(0), which measures the skin friction, "unfortunately cannot be determined by the series", suggesting that a numerical method has to be used. The unique numerical method applied requires a heuristic trial-and-error approach. Even though inconceivable, all the proposed numerical and analytical solutions add an extra boundary condition, that is

$$\frac{\partial^2 \mathrm{f}(\eta)}{\partial \eta^2}\Big)_0 = \mathrm{s} \tag{8}$$

which, specifically, requires the adoption of a mathematical technique to convert the Boundary Value Problem (BVP) defined by Equations (7) and (4) through (6) into an Initial Value Problem (IVP), as first used by Töpfer [20]. The method discussed by Conte [21] applies to both linear and non-linear problems. In certain situations, it is easy to implement, and when it converges, it is generally the most efficient method available. However, solving the Blasius equation is challenging, as it requires a variable transformation before applying the Euler method as noted by Fazio [22]. Jaguaribe [23] emphasizes a well-known point: the technique of reducing boundary value problems (BVPs) to initial value problems (IVPs) is not always applicable. Na [24] points out that for this transformation method to be applied, the boundary conditions at the initial point must be homogeneous. Klamkin [25], also

referencing Na [24], adds that while this condition is not always necessary, it is advisable to assume the existence and uniqueness of solutions for all boundary value problems (BVPs) and initial value problems (IVPs). However, this assumption has implications for the boundary conditions, and, in general, may not hold. Zeldovich and Myshkis [26], on pages 32 and 33, and Nickel [27] noted that while the boundary conditions ($u = v = 0$ at $y = 0$, and u approaches U_∞ as $y \to \infty$) ensure the existence of a solution, there is no guarantee of its uniqueness.

On the other hand, Schlichting [28] discusses the flat plate boundary layer on page 136, suggesting that **the region immediately behind the leading edge can be excluded**. As is obvious, this suggestion interferes with the definition of the boundary conditions, thereby prejudicing the mathematical solution of the problem.

The first non-null term of the series solution for the classical Blasius flat plate equation is a constant and an unknown:

One possible reason for introducing a non-standard boundary condition, as previously mentioned, is that the first nonzero term of the series expansion used to solve the Blasius equation - Equation (8) - has been treated as an unknown. It is well-known that Equation (7) was solved numerically, with the function f expressed in terms of a series, that is:

$$f(\eta) = \sum_{k=0}^{\infty} a_k \eta^k \tag{9}$$

where $k = 3j + 2$, $j = 0, 1, 2, \ldots$, $a_0 = a_1 = a_3 = a_4 = a_6 = \ldots = 0$. After applying the boundary conditions and performing some manipulations, Equation (9) is transformed into:

$$f(\alpha, \eta) = \sum_{k=0}^{\infty} \left(-\frac{1}{2}\right)^k \frac{C_k \alpha^{k+1}}{(3k+2)!} \left(\frac{\eta}{2}\right)^{3k+2} \tag{10}$$

where

$C_0 = 1$, $C_1 = 1$, $C_2 = 11$, $C_3 = 375$, $C_4 = 27897$, …

$\alpha = a_2/2$, a_2 being the first non-null term of the series solution.

It is intriguing how the primary focus in tackling the Blasius equation has always been on finding the alpha value. The limited number of natural boundary conditions has prompted the introduction of a new artificial non-conforming boundary condition, represented by Equation (8). Then, an approach is necessary: employ a mathematical technique to establish that $\alpha = f''(0) = 0.332$ (Several authors, including Sissom and Pitts [3] and Rohsenow and Choi [9], consistently refer to this value with three decimal places). This technique is associated with the production of an asymptotic solution. Noting that $f'(5) = u/U_\infty = 0.99155$, this point on the asymptotic curve represents the boundary layer limit, where $y = \delta$, and $u = U_\infty$. In other words, the approach allowed the definition of a single value of η_∞ and, consequently, a specific boundary-thickness value, δ, for the entire boundary layer.

By using a series expansion of $f(\eta)$ as outlined in Equation (9), together with Equations (1) to (6), it is possible to solve Equation (7) without adding a non-natural boundary condition. Deriving Equation (9) with respect to η, we will have:

$$f'(\eta) = \sum_{k=0}^{\infty} k a_k \eta^{k-1} \tag{11}$$

Consequently

$$f''(\eta) = \sum_{k=0}^{\infty} k(k-1)a_k \eta^{k-2} \quad (12)$$

$$f'''(\eta) = \sum_{k=0}^{\infty} k(k-1)(k-2)a_k \eta^{k-3} \quad (13)$$

Applying boundary conditions (5) and (6) results in $a_0 = a_1 = 0$. By substituting Equations (9), (12), and (13) into Equation (7), we can derive the following formulations:

$$a_5 = -\frac{{a_2}^2}{60},\ a_8 = \frac{11{a_2}^3}{20160},\ a_{11} = -\frac{5{a_2}^4}{266112},\ a_{14} = \frac{9299{a_2}^5}{2494600},\ \ldots \quad (14)$$

Where,

$$a_3 = a_4 = a_6 = a_7 = \ldots = 0 \quad (15)$$

and $\alpha = a_2$.

When *y* approaches ∞, *η* approaches η_∞, and at this limit, there is the occurrence of the potential flow zone, which means that Equation (3), affected by boundary condition (4), gives $f(\eta_\infty) = \eta_\infty$, permitting Equation (9) to be rewritten as:

$$f(\eta_\infty) = \sum_{k=2}^{\infty} a_k {\eta_\infty}^k = \eta_\infty \quad (16)$$

And due to Equation (4), Equation (11) gives:

$$f'(\eta_\infty) = \sum_{k=2}^{\infty} k a_k {\eta_\infty}^{k-1} = 1 \quad (17)$$

The combination of Equations (7), (12) and (13) yields:

$$1 - \frac{1}{15}\lambda + \frac{11}{2880}\lambda^2 - \frac{25}{133056}\lambda^3 + \frac{9299}{1117670400}\lambda^4 - \cdots = 0 \quad (18)$$

Where

$$\lambda = \alpha {\eta_\infty}^3 \quad (19)$$

From Equations (17) and (19), we have:

$$2\lambda - \frac{1}{12}\lambda^2 + \frac{11}{2520}\lambda^3 - \frac{5}{24192}\lambda^4 + \frac{9299}{1037836800}\lambda^4 - \cdots = {\eta_\infty}^2 \quad (20)$$

Equation (20) is solved using Mathcad's Release 15 root function, with two arguments and 671 terms. This calculation resulted in λ = 29.71230. From Equation (20), we find that η_∞ equals 4.69579. Consequently, Equation (19) gives $\alpha = 0.28695$, allowing the determination of the velocity distributions presented in Figure 2.

Contrary to Blasius's findings, the solution provided here is unique. The velocity in the y-direction adheres to Prandtl's [29] boundary layer concept, as $v(0) = 0$, and $v(\eta_\infty) = 0$. However, it is unusual for the x-direction velocity components within the boundary layer to exceed the free stream velocity. This fact stems from the series-expansion solution, which results in a monotonic, ascending curve derived from an odd number of series terms, rather than an asymptotic curve. In another atypical situation, the two points just before the final points of both velocity distributions, u/U_∞ and v/U_∞, do not form a continuous curve. The points preceding the last one in each situation diverge from the original curve to satisfy the boundary conditions, as shown in Figure 2. The continuity equation in its differential form is the main source of the issues.

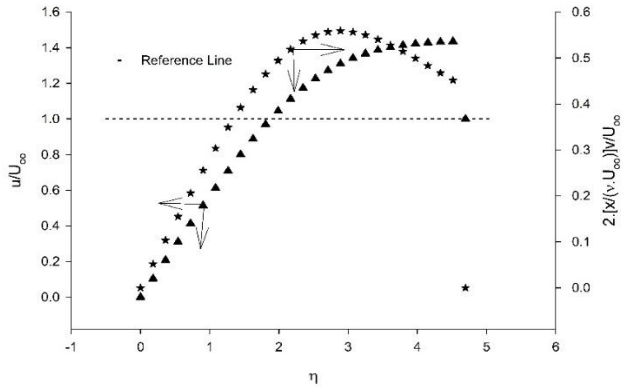


Figure 1: Velocity distributions given by Equations (2) and (3) and the series expansion (9) whose terms are given by Equation (14).

Due to the various controversies surrounding the flat-plate Blasius theory and the mistaken approach of determining the first nonzero term in the series, we developed a new formulation for the flat-plate boundary layer, which is the focus of the following discussion.

METHODS

Transforming the Partial Differential Equation (21) into an Ordinary Differential Equation

The x-direction Velocity Component, u.

Let us recall that the classical procedure to transform the partial differential equation (21) is based on defining the similarity parameter *η (*see Equation (7)) in terms of the local $u\frac{\partial u}{\partial x} + v\frac{\partial u}{\partial y} = \nu\frac{\partial^2 u}{\partial y^2}$, (21) Reynolds number raised to a constant power. This leads to the conclusion that *η*, at the limit of the boundary layer, denoted by η_∞, is a constant valid for the whole plate. To avoid such an inconvenience this work proposes to define $\eta = \eta(x, y)$ in the following manner:

$$\eta(x, y) = yx^{-\mathrm{p}(x)}\mathrm{A} \tag{22}$$

where p = p(*x*) is a nondimensional variable, and A, a function of ν and U_∞, assumes the following form:

$$\mathrm{A}(x) = \left(\frac{\mathrm{U}_\infty}{\nu}\right)^{q(x)} \tag{23}$$

where q = q(*x*).

Thus, Equation (22) turns into

$$\eta(y, x) = \frac{y}{x}\mathrm{x}^{-\mathrm{p}(x)-q(x)+1}Re_{\mathrm{x}}{}^{q(x)} \tag{24}$$

then, expressing the Reynolds local number, Re_x, as

$$Re_{\mathrm{x}} = \frac{\mathrm{U}_\infty x}{\nu} \tag{25}$$

by dimensional analysis:

$$\mathrm{p}(x) + q(x) = 1 \tag{26}$$

which means that Equation (24) becomes:

$$\eta(x, y) = \frac{y}{x} Re_{\mathrm{x}}^{1-\mathrm{p(x)}} \tag{27}$$

thus

$$\frac{\delta(\mathrm{x})}{x} = |\eta_{\infty}(x)| Re_{\mathrm{x}}^{-1+\mathrm{p}(x)} \tag{28}$$

where $\eta \to \eta_{\infty}$ when $y \to \infty$, i.e., $y \to \delta$. (In Blasius's model, η_{∞} is considered constant along the flat plate, assuming the value 5.0, and p = 0.5. Fixing those values, however, implies that δ becomes a function of *x*. Concomitant with this fact, $\delta(\mathrm{x})$ increases with $x^{0.5}$, never assuming a form of an asymptotical curve, for given values of ν and U_{∞}, which contradicts the theory.)

From Equation (27) it comes:

$$\frac{\mathrm{d}\eta(x,y)}{\mathrm{d}x} = -\frac{\eta(x,y)\mathrm{K}(x)}{x.Re_{\mathrm{x}}} \tag{29}$$

where

$$\mathrm{K}(x) = \mathrm{k}[\ln(Re_{\mathrm{x}}) - 1] \tag{30}$$

and k and b are constants, and p(*x*) is assumed to be a power function of Re_x, so that,

$$\mathrm{p}(x) = \mathrm{k}Re_{\mathrm{x}}^{\mathrm{b}} \tag{31}$$

Equation (27) also yields:

$$\frac{\mathrm{d}\eta(x,y)}{\mathrm{d}y} = \frac{\eta(x,y)}{y} \tag{32}$$

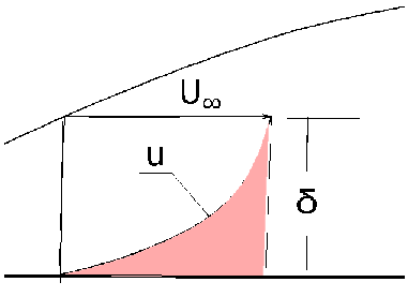


Figure 3: A portion of the boundary layer illustrating the x-direction velocity distribution and the boundary layer thickness.

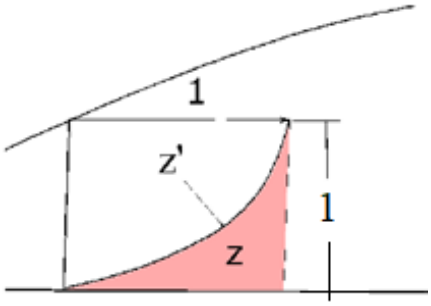


Figure 4: A section of the boundary layer illustrating the nondimensional x-direction velocity distribution, the area beneath the curve z´, and the boundary layer thickness.

Figure 3 illustrates a section of the boundary layer, emphasizing the x-direction velocity distribution and the boundary layer thickness. Similarly, Figure 4 presents the same velocity distribution in nondimensional form, along with the surface area z, derived by integrating $z_\eta(\eta)$, the first derivative of *z* with respect to η. Figure 4 serves as the basis for defining Equation (33):

$$z_\eta(\eta(x,y)) = \frac{u}{U_\infty} \tag{33}$$

The y-direction Velocity Component

The classical physical model describing the flow over a flat plate has been poorly formulated from the outset, as it did not account for a reference system justified by the presence of both kinematic and dynamic effects responsible for the formation of the boundary layer. One consequence is that the y-direction velocity component does not satisfy Prandtl's boundary-layer concept, as shown in Figure 2. Additionally, in the traditional model for Newtonian flows, the effect of viscosity is accounted for to evaluate the competition between inertia and viscous forces over a flat plate, while ignoring the direct consequences for the velocity profiles, regardless of the regime. Following a rational route implies developing both velocity components that fully satisfy Prandtl's concept.

From Equations (27), (30), (31), and (33):

$$\frac{\partial u}{\partial y} = U_\infty \frac{\eta(x,y)}{y} z_{\eta\eta} \tag{34}$$

$$\frac{\partial^2 u}{\partial y^2} = U_\infty \left(\frac{\eta(x,y)}{y}\right)^2 z_{\eta\eta\eta} \tag{35}$$

$$\frac{\partial u}{\partial x} = -U_\infty . \eta(x,y) . \frac{\partial z_\eta}{\partial \eta}\frac{\partial \eta}{\partial x} = -U_\infty . \eta(x,y) z_{\eta\eta} K(x) \tag{36}$$

where $z_\eta, z_{\eta\eta}, \text{and } z_{\eta\eta\eta}$ represent the first three derivatives of *z* with respect to η.

From Equation (27)

$$dy = \frac{y}{\eta} d\eta \tag{37}$$

The continuity equation is commonly applied in differential form, as shown in Equation (1). To examine a fluid flowing through a section of the boundary layer, we use an

Eulerian reference frame to identify disturbances that affect laminar flow. This approach allows the estimation of main effects on the fluid. Selecting an appropriate control volume around the apparatus (the plate) is crucial for evaluating the inflow's influence on the entire boundary layer, because it lets us consider the actual momentum transfer occurring at the control surface and how diminished momentum propagates into the mass of flow, decelerated by the frictional force, generating each particular boundary layer. Therefore, we can detect these overall mechanisms and results only by applying the integrated continuity equation, particularly within a representative section of the boundary layer, as shown in Figure 1. Thus, we should integrate the linear function over a finite segment of the plate (Δx) over which the mass moves. The boundary-layer edge and a section of the plate define the integration area. This process leads to Equation (38).

$$\int_0^{y'} \rho \frac{u}{U_\infty} dy.1 + \int_{x_0}^{x_1} \rho \frac{v}{U_\infty} dx.1 = \rho y'.1 \tag{38}$$

Moreover, using Equations (27) and (29) through (32), integration of Equation (38) from 0 to δ, after some mathematical manipulations, yields the new dimensionless y-direction velocity:

$$\frac{v(x,y)}{U_\infty} = \eta(x,y).p(x)(\ln(Re_x) - 1)\left(1 - z_\eta\right)Re_x{}^{p(x)-b-1} \tag{39}$$

The New Flat Plate Boundary Layer Equation

By substituting Equation (21) with Equations (29) through (33), the new equation for the flat plate boundary layer becomes:

$$\xi(x).\eta(x,y).(2z_\eta - 1)z_{\eta\eta} + z_{\eta\eta\eta} = 0 \tag{40}$$

Then, considering Equation (32), Equation (40) gives

$$\xi(x) = p(x).[1 - \ln(Re_x)]Re_x{}^{2p(x)+b-1} \tag{41}$$

To simplify the notation in the equations, from this point onward, $\xi(x)$, is denoted by ξ, $p(x)$ by p, and $\eta(x,y)$ by η.

Solving Equation (40)

The Series Expansion in λ for the Evaluation of the Solution z

To ensure alignment with the flow conditions generated by a towed object and to maintain similarity in the velocity profiles, Schlichting [28] discusses the flat plate boundary layer on page 136. As mentioned earlier, he suggests excluding the region immediately behind the leading edge. However, to accurately represent the presumed uniform flow essential to the physical model, it is necessary to characterize and describe all relevant mathematical aspects. Moreover, to ensure an adequate series solution of Equation (40) for all $y \neq 0$, two distinct conditions regarding the x-direction velocity component, *u*, are necessary:

1) for all $y \neq 0$,

$$\lim_{x^- \to 0} u = U_\infty$$

2) for all *x*,

$$\lim_{y\to\delta} u = \mathrm{U}_\infty$$

As a result, the only series that can fulfill these requirements is

$$\mathrm{z}(\eta) = \mathrm{a}_2\eta^2 + \sum_{\mathrm{k}=3}^{\mathrm{n}} \mathrm{a}_\mathrm{k}\eta^\mathrm{k} \quad (42)$$

where,

$$\mathrm{a}_2 = \frac{1}{2\eta_\infty}. \quad (43)$$

Therefore,

$$\mathrm{z}_\eta(\eta_\infty) = 1 + \sum_{\mathrm{k}=1}^{\frac{\mathrm{N}-1}{2}} \mathrm{k}\mathrm{a}_{(2\mathrm{k}+1)}{\eta_\infty}^{\mathrm{k}-1} = 1 \quad (44)$$

to satisfy condition (4), where $a_0 = a_1 = 0$, which means that:

$$\mathrm{z}_\eta(\eta_\infty) = 1 \quad (45)$$

Then, from Equations (42) and (43):

$$z_{\eta\eta}(\eta) = \frac{1}{\eta_\infty} + \sum_{\mathrm{k}=3}^{\mathrm{N}} \mathrm{k}(\mathrm{k}-1)\mathrm{a}_\mathrm{k}\eta^{\mathrm{k}-2} \quad (46)$$

$$z_{\eta\eta\eta}(\eta) = \sum_{\mathrm{k}=3}^{\mathrm{N}} \mathrm{k}(\mathrm{k}-1)(\mathrm{k}-2)\mathrm{a}_\mathrm{k}\eta^{\mathrm{k}-3} \quad (47)$$

The two other natural boundary conditions are:

$$z(0) = 0, \quad (48)$$

$$z_\eta(0) = 0. \quad (49)$$

Considering Equations (42), (44), and (47) and conditions (45), (48), and (49), we come to the following:

$$\xi + 6\mathrm{a}_3 + 24\mathrm{a}_4\,\eta_\infty + (6\xi\mathrm{a}_3 + 60\mathrm{a}_5){\eta_\infty}^2 + (12\xi\mathrm{a}_4 + 120\mathrm{a}_6){\eta_\infty}^3 + (20\xi\mathrm{a}_5 + 210\mathrm{a}_7){\eta_\infty}^4 + \cdots = 0 \quad (50)$$

Upon evaluating the terms in Equation (50), we conclude that

$$a_4 = a_6 = a_8 = a_{10} = a_{12} = \ldots = 0 \quad (51)$$

The odd terms are provided by:

$$\mathrm{a}_{2\mathrm{j}+3} = (-1)^{\mathrm{j}+1}\frac{2^\mathrm{j}\mathrm{j}!}{(2\mathrm{j}+3)!} \quad (52)$$

j = 0, 1, 2, …

Therefore, Equation (50) is rewritten as follows:

$$-\frac{1}{2} + \frac{\eta_\infty^2}{12}\xi - \frac{\eta_\infty^4}{90}\xi^2 + \frac{\eta_\infty^6}{840}\xi^3 - \frac{\eta_\infty^8}{9450}\xi^4 + \frac{\eta_\infty^{10}}{124740}\xi^5 - \cdots = 0 \quad (53)$$

That is,

$$-\frac{1}{2} + \frac{1}{12}\lambda - \frac{1}{90}\lambda^2 + \frac{1}{840}\lambda^3 - \frac{1}{9450}\lambda^4 + \frac{1}{124740}\lambda^5 - \cdots = 0 \quad (54)$$

where,

$$\lambda = \eta_\infty^2\xi \quad (55)$$

Using Mathcad's Release 15 root function with four arguments and the series with 301 terms, the evaluation gives λ = 116.74438. It is important to note that in this case, only positive and real values are considered valid solutions. According to the Fundamental Theorem of Algebra, every non-constant polynomial with complex coefficients has at least one root in the complex numbers, as noted by Fine and Rosenberger [30]. This finding is also consistent with Descartes's rule of signs, as discussed by Meserve and Klein [31]. Therefore, the polynomial in Equation (54) has exactly one real root when it contains an even number of terms, allowing the identification of a valid root λ.

The Coefficient a_2

As commented, Equation (8), though used as a boundary condition to solve the flat plate equation, is an unsupported mathematical recourse. It is an artificially imposed fourth boundary condition for 'solving' Blasius's third-order ordinary differential equation for a flat plate. In the context of the shooting method, 's' represents a guess, as noted by Nellis and Klein [32]. This leads to mathematical inconsistencies and results in an incorrect solution. A major frustration occurs when it is necessary to admit that the 'solution' is not unique. In section 7.6, titled "Uniqueness of the Blasius Solution," Van Dyke [33] concludes—from a mathematical perspective—that the solution to Equation (7.17), which corresponds to Equation (7), is not unique. In addition, the classical procedure treats the first non-zero coefficient of its series solution, a_2, as a constant and an unknown. This is a rhetorical error. It has attracted innovative mathematical and physical mechanisms that bring more complexity than clarity. Thus, quantifying its value in the Blasius solution became the primary goal. The immediate consequence is that the values of α, the non-numerical coefficient present in the classical series solution represented by f(α), as well as the stretch factor, η, at infinity, and the boundary layer thickness are all considered constant across the entire plate. All these inaccuracies surrounding the flow behavior have led to rough formulations and approaches. Key concepts in this context include displacement thickness, δ^*, and momentum thickness, δ_1. In addition, the boundary layer thickness is defined somewhat arbitrarily as the point at which the velocity reaches 99% of the free stream velocity. These ambiguities have led to the use of inconsistent fixed factors in classical expressions. For example, correlations for boundary-layer thickness yield values such as 5.0 or 4.64, whereas the traditional value for the local skin friction coefficient is 0.332.

Insensible to these questions, the specialized literature continues to present both traditional and modern numerical solutions, with authors replicating all of Blasius's questionable results using numerical data, plots, and figures. Contributors to these ongoing issues include Lai & Milin [34]; Parlange, Braddock, and Sander [35]; Shoukat, Yaseen [36]; Ahmad and Al-Barakati [37]; Marinca and Marinca [38]; Pakdemirli [39]; Asaithambi [40]; Nasser and Shrif [41]; and Santos, Santiago, and Bodstein [42], among others. These controversies surrounding the flat plate boundary layer theory have undoubtedly hindered the advancement of fluid mechanics as a precise field of study.

It is important to note that the first term of the series solution associated with Equations (42) and (43) arises from a natural geometric configuration. That is, when $\eta \to 0$

$$2a_2 = z_{\eta\eta}(0), \tag{56}$$

where a_2 is a function of the tangent of angle α(x), where α(x) is formed by the tangent to the u curve and a line perpendicular to the plate that intersects at a common point on the curve and the plate. Thus,

$$2a_2(x) = \beta(x) = \tan(\alpha(x)) \tag{57}$$

And following from Equation (43)

$$\eta_\infty(x) = \frac{1}{\tan[\alpha(x)]} \tag{58}$$

where

$$0 \leq \alpha(x) < 0.7\pi \tag{59}$$

This maximum limit for α(x) given by Equation (59) is linked to the critical Reynolds number considered in our model, namely 500,000, with a kinetic viscosity of 1.263 x 10^{-4} m^2/s. Thus, for a length of L = 1 m, Re_L = Re_C, where the free stream velocity, U_∞, is 63.15 m/s. Physically, the angle α(*x*) is a result of the viscosity effect and is a function of *x*. The role of this angle becomes crucial for the correct solution of the Blasius equation; it intervenes directly in the definition of u and v velocity components, and the parameter p, and is a key element in the evaluation of the regime transition zone, thus defined as

$$\alpha(x) \equiv c\frac{\pi}{2}\frac{x.U_\infty}{\nu.Re_C} \tag{60}$$

where, c < 1.

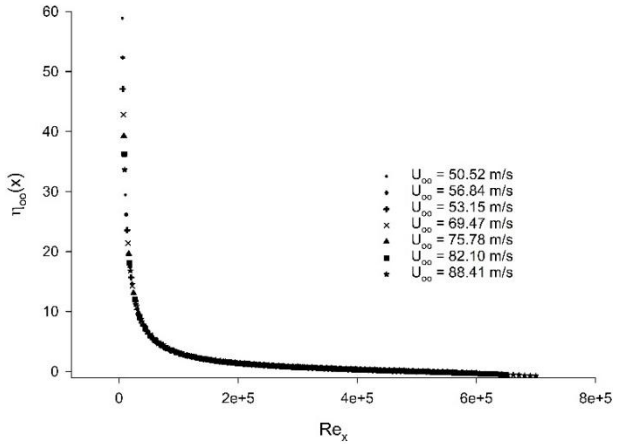


Figure 5: $\eta_\infty(x)$ in function of Re_x for seven values of the free stream velocity.

Equation (58) causes a major change in the theory of the flat plate boundary layer. As we know, the stretching function, η, originally played a key role in transforming the partial differential equation into an ordinary differential equation, appearing as a positive factor. An immediate consequence of this is that, in classical theory, it is not possible to explain reversed flow over a flat plate. However, it occurs, as evidenced by experimental measurements reported by Willert [43] or by direct numerical simulation (DNS) studies by Spalart and Strelets [44]. Thus, from Equations (58), (59), and (60), by admitting in Equation (60) that c = 0.999, it is possible to plot $\eta_\infty(x)$ as a function of the local Reynolds number, Re_x, as shown in Figure 5. In Figure 5, the critical Reynolds number, Re_C, was assumed to be

500,000, In Figure 5, independent of the value of the free stream velocity, the points remain on the monotonic curve. For values of Re_x > 500.000, $\eta_\infty(x)$ becomes negative, indicating that the main flow reverses direction and that, inside the separation zone, the near-wall fluid circulates backward.

This paper presents a theory based on an ideal uniform, parallel flow over a smooth, perfect surface, in which the velocity profiles of a Newtonian flow, depending on the circumstances, exhibit inflection points. Nevertheless, the flow is not undergoing a receptivity process, as considered by Bhoraniya, Swaminathan and Narayanan [45], nor is it influenced by environmental forcing, as discussed by Morkovin and Reshotko [46].

Evaluation of Factor p

Equations (41) and (55) give:

$$\frac{\lambda}{\eta_\infty^2} = p[\ln(Re_x) - 1]Re_x^{2p-2+b} \tag{61}$$

Therefore,

$$0 = \ln(p) + \ln[]\ln(Re_x) - 1] + (2p - 2 + b)\ln(Re_x) - \ln\left(\frac{\lambda}{\eta_\infty^2}\right) \tag{62}$$

Using the Mathcad Release 15 root function with four arguments and 301 terms, we solved Equation (62) and then plotted the graph shown in Figure 6. It displays the behavior of p(x) as a function of the local Reynolds number for seven different values of U_∞. It becomes evident that p increases up to the limit of the laminar zone. Suddenly starts decreasing, showing striking sensitivity in capturing the variations of the regime transition.

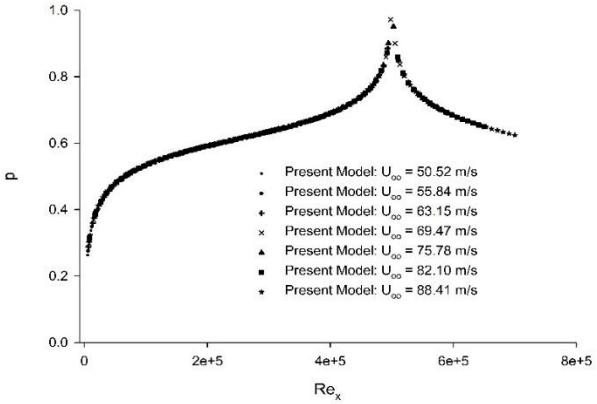


Figure 6: Distribution of p(x) in function of Re_x, considering seven different values of the free stream velocity.

OTHER RESULTS AND COMMENTS

The Boundary Layer Thickness, δ(x)/x

Equation (28) allows the calculation of $\delta(x)/x$. By comparing Equation (28) to the traditional Blasius expression, it becomes clear that in the Blasius equation, 5.0 replaces $\eta_\infty(x)$, and 0.5 replaces $1 - p(x)$, resulting in the well-known expression:

$$\frac{\delta}{x} = \frac{5.0}{Re_x^{0.5}} \tag{63}$$

Since the boundary layer thickness represents a distance, it must be nonnegative by definition. Therefore, Equation (28) uses the modulus of the stretcher function. Figure 6 displays curves derived from Equations (63) and (28) for a plate divided into 301 stages, considering seven different free stream velocity magnitudes: U_∞ = 50.52 m/s, 56.84 m/s, 63.15 m/s, 69.47 m/s, 75.78 m/s, 82.10 m/s, and 88.41 m/s. As demonstrated, changes in the free stream velocity do not alter the value of the corresponding points for a determined local Reynolds number. The values of δ/x from the present model are slightly larger than those from Blasius in the region where Re_x < 48,640.

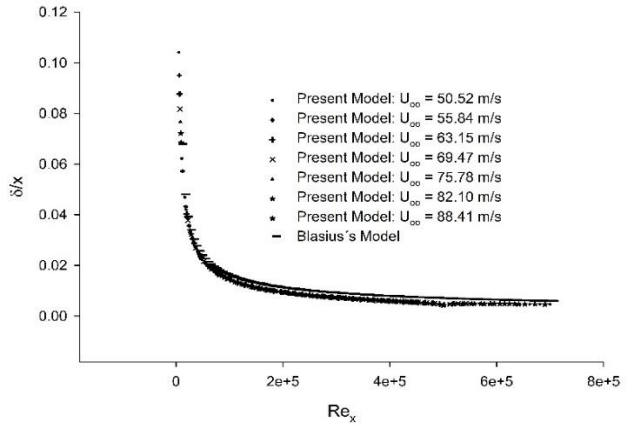


Figure 7: Results for the boundary layer thickness, δ/x, related to seven free stream velocities, calculated using the present model and Blasius's

On the other hand, they seem more sensitive to the approximation of the leading edge than the ones calculated by Blasius. Clayton et al. [47], noting that the values of $\frac{\delta}{x}$ do not increase as expected when x approaches zero (page 288), stated that "experimental evidence indicates that the Blasius solution is valid except very close to the leading edge of the plate." Both curves seem quite parallel. It is possible to see that the portion in the transition to the turbulent zone presents a small accent relative to the one in the laminar region.

The Local Skin Friction Coefficient, $C_{f,x}$

By definition,

$$C_{f,x} = \frac{\tau_{w,x}}{\frac{\rho U_\infty^2}{2}} = \frac{\mu\left(\frac{\partial u}{\partial y}\right)_{y=0}}{\frac{\rho U_\infty^2}{2}} \tag{64}$$

From Equations (64) and (34), it is possible to deduce Equation (65).

$$C_{f,x} = \frac{2}{z_{\eta\eta}(0)} . Re_x^{-p(x)} \tag{65}$$

Rewriting Equation (65) and considering p(x) = 0.5 and $z_{\eta\eta}(0) = 0.332$, it comes to the expression for the local skin friction coefficient related to the flat plate, due to Blasius:

$$\frac{C_{f,x}}{2} = 0.332 Re_x^{-\frac{1}{2}} \quad (66)$$

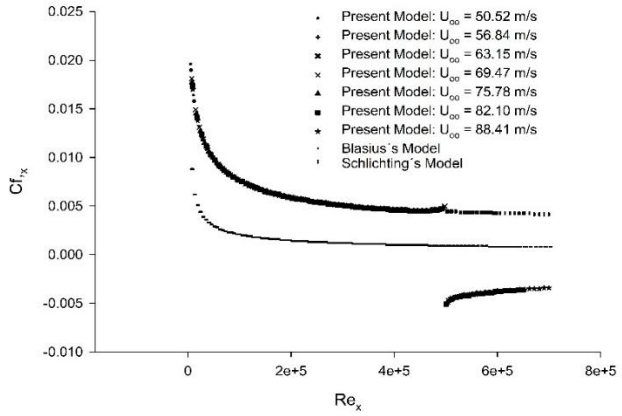


Figure 8: Local skin friction coefficient calculated by Equation (65)— present model— by Equation (66)—Blasius's [1] model; and by Schlichting's [28] correlation, Equation (67), expressed in a semi-log scale, considering seven stream velocity values.

Figure 7 shows the local skin friction curves as a function of the local Reynolds number on a semi-log scale, using Equations (65) and (66) for the present work and Blasius's model, respectively, and the empirical correlation given by Equation (67), due to Schlichting [28], valid for $5 \times 10^5 < Re_x < 10^7$

$$\frac{C_{f,x}}{2} = \frac{0.0592}{Re_x^{1/5}} \quad (67)$$

Equation (67) is valid for smooth, flat plates with turbulent boundary layers. Figure 8 shows the local skin friction coefficient as a function of the local Reynolds number, for seven different free stream velocities. As noted, the curves of the present model and the Blasius model are quite parallel, but the present model shows higher values, demonstrating sensitivity to the regime change. As is well known, Blasius's curve does not respond to the transition to the turbulent region. As commented by Katopodes [48] (page 670), "…the solution of Blasius for laminar boundary layers does not extend to turbulent boundary layers…" It is worth noting that all the points associated with Equation (67) in the turbulent domain appear to be a continuation of those of the present model, except for those altered by sensitivity to the turbulent zone.

Figure 9 shows local skin friction data published by Fürst [49]. The author compare their k-kL-ω laminar/turbulent transition model with other theoretical models and with results from the classical ERCOFTAC experimental test cases published by Savill [50]. These tests describe the local coefficient in boundary-layer flow on a flat plate with various free stream turbulence levels: T3A (U_∞ = 5.4 m/s), T3B (U_∞ = 9.4 m/s), and T3A- (U_∞ = 19.8 m/s). Ignoring the curve formats in Figures 8 and 9, we can see a clear agreement between the experimental values and those of the present model in the region $2 \times 10^5 < Re_x < 5 \times 10^5$. However, we cannot compare data in the transient zone because the values in Figure 9 are not related to reversed flow. However, data in the transient zone cannot be compared because the values in Figure 9 are not related to reversed flow. Moreover, the present model is unlikely to agree with experimental data, since most experimental transition studies

require adaptations and added components (e.g., tripping devices), resulting in a non-spontaneous regime transition with adverse effects. In particular, in the experiments referred to, conducted in a closed-type wind tunnel, both the upstream and downstream airfoils were artificially equipped with 44 and 40 static pressure holes, respectively, each 0.8 mm in diameter. Additionally, as Lee and Kang [52] noted, the leading edge thickness makes it difficult to obtain accurate data over the flat plate.

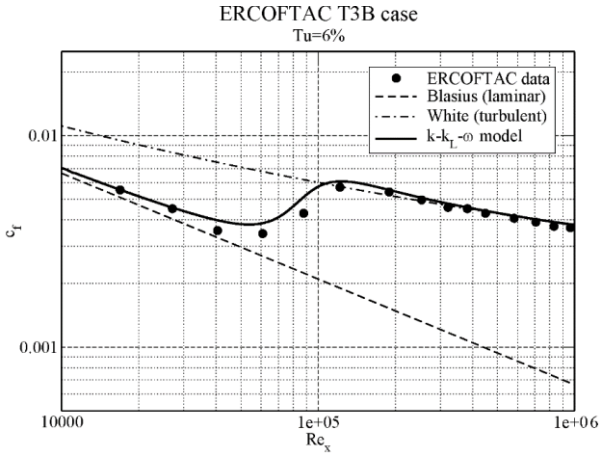


Figure 9: Plot due to Fürst [49] presenting curves based on the (k-kL-ω) model and compared with those from Blasius [1], White [51], and the ERCOFTAC experimental data, on local skin friction.

Nondimensional Velocity Components

The Nondimensional x-direction Velocity u/U∞

The correlation for the nondimensional x-direction velocity component, u/U_∞, comes from Equations (33) and (44), yielding:

$$\frac{u}{U_\infty} = \frac{\eta}{\eta_\infty} \tag{68}$$

And due to Equation (58), Equation (68) may be written as:

$$\frac{u}{U_\infty} = \eta \tan[\alpha(x)] \tag{69}$$

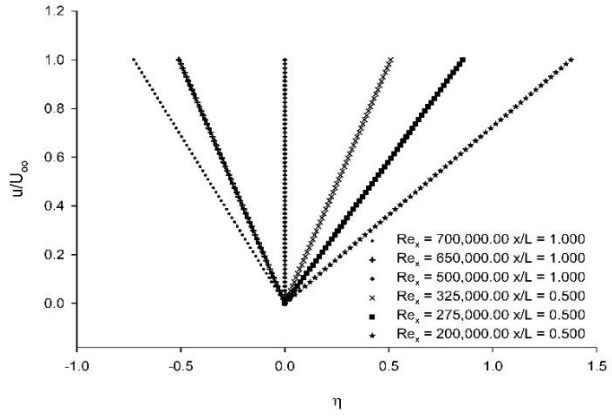


Figure 10: Nondimensional x-direction velocities in the laminar and turbulent zone.

Figure 10 shows the distribution of the nondimensional x-direction velocity, u/U_∞, within the boundary layer, mapped in terms of η and associated with the local Reynolds number, Re_x, as well as their position along the plate. The local Reynolds number varies with the free stream velocity, U_∞, and — these velocity profiles show kinematic similarity, consistent with Blasius's classical formulation. Notably, at the same location, x/L, the angle between the line representing u/U_∞ and the x-axis steepens as the local Reynolds number increases. This increase indicates a greater likelihood of a regime change. In fact, at x/L = 1.0 and Re_x = 500,000, the curve becomes a perpendicular line parallel to the y-axis. When $Re_x > Re_C$, the points fall to the left of this mentioned vertical line, indicating that the flow is no longer laminar.

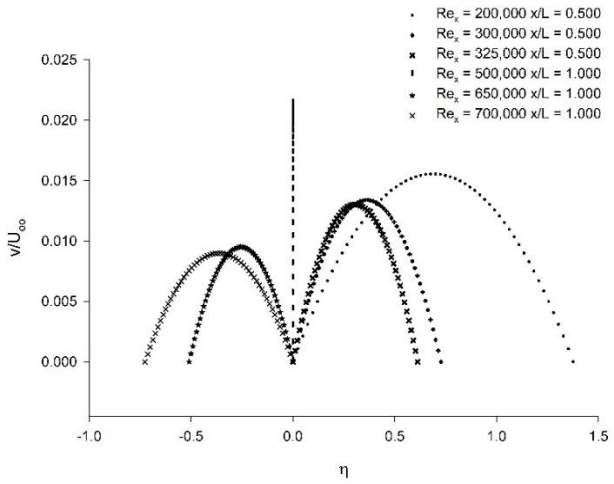


Figure 11: Nondimensional velocity distribution in the y-direction at various points along the plate.

Figure 11, similar to Figure 10, illustrates the behavior of the nondimensional y-direction velocity, v/U_∞, as a function of η, in the laminar and turbulent zones, for some Reynolds numbers. In contrast to the typical y-direction velocity profiles described by Blasius, as discussed in sources such as Rohsenow and Choi [9] or Puttkammer [53], the profiles shown in Figure 11 adhere to Prandtl's boundary layer theory. This fact becomes evident because, at the plate and within the boundary layer limit, the condition $v/U_\infty = 0$ is satisfied. Furthermore, for Re_x > 500,000, the profiles lie in the second quadrant (see Figure 11) and always adhere to the Prandtl's boundary layer principle. Furthermore, it demonstrates the ongoing regime transition starting when the stretch function becomes null and the presence of reverse flow.

Effects of Vorticity in the Boundary Layer

Lighthill and Rosenhead [54] and Morton [55] argue that momentum mechanisms alone are sufficient to explain local behavior within a boundary layer. They emphasize that understanding vorticity is essential for comprehending the overall dynamics of the boundary layer. In this context, Cottet and Koumoutsakos [56] note that it is often more beneficial to describe dynamic events in a flow by focusing on the evolution of the vorticity field. This perspective is particularly relevant given the limitations of applying explicit velocity components in theory, which persist even in the two-dimensional flat-plate boundary layer.

These restrictions motivated researchers, such as Dushane [57], Hald [58], Zhang [59], Chorin [60], and others, to simulate vorticity generation numerically. Chorin [58] solved the differential equations without boundaries. For this, he partitioned the vorticity into a sum of discrete blobs. This procedure highlights the complexities involved in treating boundary layers with vorticity using numerical techniques. However, if one opts for the traditional yet complicated application of the Biot-Savart law, it presents additional difficulties. Specifically, this approach necessitates integrating viscous effects into a Lagrangian formulation, which can lead to a loss of accuracy due to the distortion of computational elements within that framework, as noted by Barba, Leonard, and Allen [61]. According to Morton [55], all the problems can be addressed using classic conservation equations, which means that descriptions of fluid motion need not be expressed in terms of vorticity. However, he suggests that using vorticity is beneficial for understanding several significant and straightforward conservation relationships. These relationships provide a powerful alternative physical basis for discussing complex three-dimensional flows. Morton [55] also emphasizes that boundaries in homogeneous fluids are the source of all vorticity. He notes, nevertheless, that Batchelor [62] is one of the few authors who recognize the importance of solving vorticity equations in conjunction with boundary conditions.

Vorticity, Two-Dimensional Exact Equations

For potential flow over a cylinder or a flat plate, multiple solutions can arise depending on the intensity of the circulation, as noted by Carlton [63]. It is well-known that at zero incidence, the flow remains predominantly attached and symmetric, resulting in minimal or no vortices unless perturbations are present. Generally, for a flat plate or a cuspid trailing edge, the vorticity mechanism can be determined by applying an unsteady Kutta condition, based on the physical sense that flows cannot turn around a sharp edge. Xia and Mohseni [64] argue that determining the angle of an airfoil with a finite-angle trailing edge is challenging. To address this issue, they calculated the angle using the fundamental conservation laws of mass and momentum, along with a condition derived from Kelvin's circulation theorem.

Nevertheless, as noted by Hemati et al. [65], many vorticity-generation models based on the Kutta condition at small angles of attack and in the absence of the leading edge vortex (LEV) reasonably predict the circulatory forces and moments on the wing. The accuracy of predictions decreases significantly when working with amplified attack angles, especially when the LEV plays a crucial role in the process. However, we can simplify these complex methods and imprecise solutions by establishing clear relationships for the velocity components. It is possible to formalize this concept using the new boundary layer concept for flat plates, as presented here and illustrated in the following two-dimensional case.

Equations (39) and (68) represent the solutions for the velocity components in the x- and y-directions, respectively. Additionally, by applying Equations (27), (34), (36), (43), and (47), we can explicitly calculate the vorticity component in Cartesian coordinates, denoted by ζ, for two-dimensional flow using Equation (70):

$$\zeta = \frac{\partial v}{\partial x} - \frac{\partial u}{\partial y} \tag{70}$$

where:

$$\frac{\partial v}{\partial x} = \frac{\mathrm{U}_\infty}{x}\{A1(x)[Z1(x) + (\ln Re_\mathrm{x} - 1)(A2(x) + Z2(x))]\} \quad (71)$$

$$A1(x) = {Re_\mathrm{x}}^{p(x)-b-2}.\,\mathrm{p(x)}.\,\eta(x,y)$$

$$A2(x) = [p(x)(b\ln Re_\mathrm{x} + 1) - b - 1]Z1(x)$$

$$Z1(x) = Re_\mathrm{x}(1 - \mathrm{z}_\eta(x))$$

$$\mathrm{Z2}(x) = \mathrm{z}_{\eta\eta}(x)\,\eta(x,y){Re_\mathrm{x}}^{-b}\,(\ln Re_\mathrm{x} - 1)$$

$$\mathrm{b} = 1/10$$

and

$$\frac{\partial u}{\partial y} = \frac{\mathrm{U}_\infty}{x}\mathrm{z}_{\eta\eta}(x){Re_\mathrm{x}}^{1-p(x)} \quad (72)$$

Equation (70), together with Equations (71) and (72), is a powerful tool that sheds light on the vortex impact on the boundary layer. Figure 11 shows curves of vorticity formation as a function of η corresponding to designated x/L locations for some Re_x. Although Equation (71) may appear cumbersome, we can ignore it because v is smaller than u, and the y-direction gradients (normal to the surface) are much steeper than the x-direction gradients. This means we can obtain the total vorticity from Equation (72) alone, although in our calculation we used both terms. Figure 11 helps us better understand vorticity behavior in the boundary layer. From it, we see that the resulting vorticity field consists of one part attached to the plate and another, detached, shedding into a region of vorticity away from the surface, that is, into a wake. This conclusion is evident because the coupling between shearing and compression processes weakens as Re increases. Additionally, at small Re, vorticity diffusion prevails, as shown in Figure 11 and noted by Wu et al. [19].

As is well known, the vortices strongly influence the near-wall velocity gradient; thus, they can create regions of high skin friction or produce low or even reversed skin friction, resulting in near-wall flow reversal or separation and determining the conditions for turbulence to exist, which, in certain applications, requires reduction or suppression. For example, Du and Karniadakis [66] show that near-wall streaks may undergo large reductions in shear stress via a transverse traveling wave. Figure 11, supplemented by Figure 8, shows how the vortex field transforms as the free-stream velocities and their locations on the plate change. For example, at higher Reynolds numbers (Re > 500,000), the attached and free vortex layers approximate a vortex sheet, as theory predicts. Consequently, this produces hydrodynamic instabilities, transition, and the already-mentioned turbulence, as Figure 8 clearly shows.

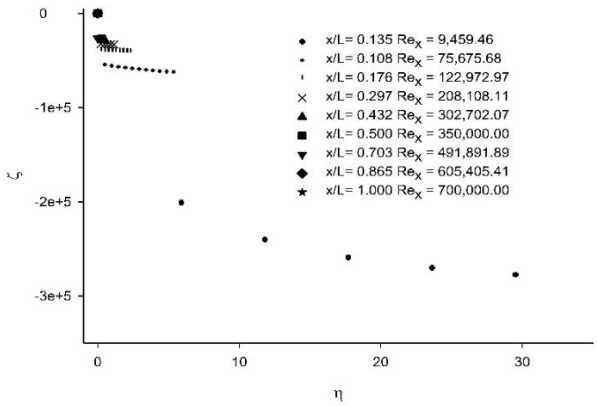


Figure 11: Vortex formation along η at different plate locations, x/L, and for eight local Reynolds numbers.

CONCLUSION

Blasius's theoretical framework and solution for the boundary layer over a flat plate challenge fundamental mathematical and physical principles. This foundational concept has influenced the development of boundary layer theory for over a century. It remains relevant today, despite contradicting established principles of integral calculus and conventional approaches to fluid motion. Fortunately, addressing some of this paradigm's shortcomings is not overly complex.

The key insight is that the first nonzero term in the series solution depends on viscosity, which is a determinant for the correct solution of Blasius's equation. This understanding, together with the use of the Eulerian reference frame, enables accurate determination of both velocity components. On the other hand, the classical definition of the similarity parameter η in terms of the local Reynolds number raised to a constant must be abandoned because it implies setting δ and η_∞ as unique values valid for the entire plate. Basically, avoiding those inconsistencies, we come to the following:

1. The deduction of a new equation for the flat plate boundary layer, which is compatible with Prandtl's boundary layer concept and capable of better describing the uniform flow advancing over a flat plate.
2. An easier understanding of how viscosity affects the transition regime, without the need to introduce environmental forcing associated with small-disturbance waves (often referred to as Tollmien-Schlichting waves), as discussed by Cousteix and Cebeci [67]. It also excludes, in the theoretical domain, the need to use the simplified en-method, mentioned by Roberts, Correia, Finnis and Knowles [68].
3. Analyses of the vorticity behavior within the flat plate boundary layer without relying on numerical simulations, the Kutta condition, the Biot-Savart law, or the incorporation of viscous effects into a Lagrangian formulation, at least considering the two-dimensional case.
4. The recognition, in emerging trends in experimental studies on regime transitions, of emphasizing a shift away from highly controlled flows, avoiding instrumentalizing

them to the point of completely altering the real natural flow, and avoiding artificial planned disturbances in suitably adapted wind tunnels.

Data Availability

All data supporting the discussions and conclusions of this paper are found in the References.

Conflicting Interests

The author has declared that no conflicting interests exist.

Funds

This work has not received any grant from any organization.

REFERENCES

1. Blasius, Heinrich. (1907) Grenzschichten in Flüssigkeiten mit kleiner Reibung. Druck von BG Teubner.
2. M. Van Dyke, (1975) “Perturbation methods in fluid mechanics/annotated edition,” NASA STI/Recon Technical Report A, vol. 75.
3. L. Sissom and D. Pitts (1972) Elements of Transport Phenomena. 1972.
4. E. L. Houghton, P. W. Carpenter, Steven Collicott, Daniel Valentine (2016) Aerodynamics for Engineering Students 7th Edition, Butterworth-Heinemann.
5. A. Guran, J. Gwinner (2012) An Enhanced Numerical Solution of Blasius Equation By Means Of The Method Of Differential Quadrature. 18th International Conference. Engineering Mechanics 2012. Svratka, Czech Republic, May 14 – 17.
6. Kármán, Th V. (1921) "Über laminare und turbulente Reibung." ZAMM-Journal of Applied Mathematics and Mechanics/Zeitschrift für Angewandte Mathematik und Mechanik 1.4: 233-252.
7. Von Kármán, Th. (1946) "On laminar and turbulent friction.".
8. Jaguaribe, Emerson Freitas (2024) A Model Built on Principles and Concepts that Address Discrepancies in the Classical Flat Plate Boundary Layer Theory. COJ Reviews & Research Volum4 Issue5 ISSN 2639-0590 *DOI: 10.31031/COJRR.2024.04.000598* October 03.
9. W. M. Rohsenow and H. Y. Choi (1961) Heat, mass, and momentum transfer. Prentice hall.
10. Pritchard, Philip J., and John W. Mitchell (2016) *Fox and McDonald's introduction to fluid mechanics*. John Wiley & Sons.
11. Welty, James, Gregory L. Rorrer, and David G. Foster (2020). Fundamentals of momentum, heat, and mass transfer. John Wiley & Sons.
12. Bennett, Carroll O., and John Earle Myers (1982) "Momentum, heat, and mass transfer." (No Title).
13. E. Jaguaribe (1995) “Rethinking von Kármán’s solution of the laminar flat plate boundary layer,” in Asian Congress of Fluid Mechanics, 6th, Singapore, pp. 334–339.

14. Jaguaribe EF. (2020) Conflicting aspects in the flat plate boundary layer conventional solution. Math Probl Eng. 2020:1-8.

15. Jaguaribe EF (2021) Conflicting aspects in the flat plate boundary layer conventional solution, Book Chapter. Prime Archives in Applied Mathematics. 2nd ed Shaikhet L, editor, Vide Leaf, ISBN: 978-81-953047-0-7 March 03.

16 Pohlhausen, Karl (1921) "Zur näherungsweisen integration der differentialgleichung der laminaren grenzschicht." ZAMM-Journal of Applied Mathematics and Mechanics/Zeitschrift für Angewandte Mathematik und Mechanik 1.4 (1921): 252-290.

17. Pohlhausen, Karl The approximate integration of the differential equation for the laminar boundary layer (1965) Department of Aerospace Engineering, University of Florida.

18. E. Weinan (2000) “Boundary layer theory and the zero-viscosity limit of the Navier-Stokes equation,” Acta Mathematica Sinica, vol. 16, no. 2, pp. 207–218.

19. Wu, Jie-Zhi, Hui-Yang Ma, and M-D. Zhou. Vorticity and vortex dynamics. Springer Science & Business Media, 2007.

20. C. Töpfer (1912) “Bomerkungen zu dem aufsatz von h. Blasius, “grenzschichten in flüssigkeiten mit kleiner reibung,” Z. Math. u. Phys. 60, 397–398.

21. S. D. Conte (1965) Elementary Numerical Analysis An Algorithm Approach, p. 268. McGraw-Hill.

22. R. Fazio (2013) “Blasius problem and Falkner–Skan model: Töpfer’s algorithm and its extension,” Computers & Fluids, vol. 73, pp. 202–209.

23. Jaguaribe EF (2022) The flat plate boundary layer equation under Blasius restrictions with a unique solution. Math Probl Eng:1-9.

24. T. Y. Na (1967) “Transforming boundary conditions to initial conditions for ordinary differential equations,” SIAM review, vol. 9, no. 2, pp. 204–210.

25. M. S. Klamkin (1970) “Transformation of boundary value problems into initial value problems,” Journal of Mathematical Analysis and Applications, vol. 32, no. 2, pp. 308–330.

26. I. B. Zeldovich and A. D. Myshkis (1976) Elements of applied mathematics. Mir.

27. K. Nickel (1973) “Prandtl’s boundary-layer theory from the viewpoint of a mathematician,” Annual Review of Fluid Mechanics, vol. 5, no. 1, pp. 405–428.

28. Schlichting, H., and K. Gersten. "Boundary-Layer Theory New York: MacGraw Hill." (1979).

29. Prandtl, Ludwig (1935) "The mechanics of viscous fluids." Aerodynamic theory: 34-208.

30. Fine, Benjamin, and Gerhard Rosenberger (1997) The fundamental theorem of algebra. Springer Science & Business Media.

31. Meserve, Bruce Elwyn (1982) Fundamental concepts of algebra. Courier Corporation, 1982.

32. Nellis, Gregory, and Sanford Klein (2008) Heat transfer. Cambridge university press, 2008.

33. M. Van Dyke, “Perturbation methods in fluid mechanics/annotated edition,” NASA STI/Recon Technical Report A, vol. 75, 1975.

34. S, A. L., & Milin, M. (2022). Accurate benchmark results of Blasius boundary layer problem using a leaping Taylors series that converges for all real values. *ArXiv*. https://arxiv.org/abs/2204.02215

35. Parlange, J. Y., R. D. Braddock, and G. Sander. "Analytical approximations to the solution of the Blasius equation." Australasian Conference on Hydraulics and Fluid Mechanics (7th: 1980: Brisbane, Qld.). Barton, ACT: Institution of Engineers, Australia, 1980.

36. Shoukat, Z., Siddiqui, A. A., Yaseen, M. H., Khan, M. I., Abdullaeva, B. S., Waqas, M., & Gupta, M. (2024). An approximate solution of the Blasius problem using spectral method. *Partial Differential Equations in Applied Mathematics*, *11*, 100896. https://doi.org/10.1016/j.padiff.2024.100896

37. Ahmad, Faiz, and Wafaa H. Al-Barakati (2009) "An approximate analytic solution of the Blasius problem." Communications in Nonlinear Science and Numerical Simulation 14.4 (2009): 1021-1024.

38. Marinca, Bogdan, and Vasile Marinca (2023) "Analytical approximation solution of nonlinear Blasius problem." The Romanian Journal of Technical Sciences. Applied Mechanics. 65.1 (2020): 15-27.

39. Pakdemirli, Mehmet (2023) "Analytical Solutions of the Blasius Equation by Perturbation Iteration Method." Proof 3 (2023): 100-107.

40. Asaithambi, A. (2016) "Numerical solution of the Blasius equation with Crocco-Wang transformation." Journal of Applied Fluid Mechanics 9.5 (2016): 2595-2603.

41. Algaidy, Nasser, and Ali El Shrif (2023) "Numerical simulation of the laminar boundary layer flow over a flat plate." DOI: 10.59743/jau.v8i4.1935.

42. Santos, Helaine C., Victor S. Santiago, and Gustavo CR Bodstein. "VORTEX METHOD SIMULATION OF BLASIUS' FLAT-PLATE BOUNDARY LAYER (2014)" Computational Thermal Sciences: An International Journal 6.6.

43. Willert, Christian, et al. "Experimental evidence of near-wall reverse flow events in a zero pressure gradient turbulent boundary layer." *Experimental Thermal and Fluid Science* 91 (2017): 320-328.

44. Spalart, Philippe R., and Michael Kh Strelets. "Mechanisms of transition and heat transfer in a separation bubble." *Journal of Fluid Mechanics* 403 (2000): 329-349.

45. Bhoraniya, Rameshkumar, Gayathri Swaminathan, and Vinod Narayanan. "Global Stability Approach." Global Stability Analysis of Shear Flows. Singapore: Springer Nature Singapore, 2023. 11-40.

46. Morkovin, M. V., and E. Reshotko (1990) "Dialogue on progress and issues in stability and transition research." Laminar-Turbulent Transition: IUTAM Symposium Toulouse/France September 11–15, 1989. Berlin, Heidelberg: Springer Berlin Heidelberg.

47. Clayton, T. Crowe, F. E. Donald, and A. R. John (2002) "Engineering fluid mechanics." (2002): 15-60.

48. Katopodes, Nikolaos D (2018) Free-surface flow: environmental fluid mechanics. Butterworth-Heinemann.

49. Fürst, Jirí. "Numerical simulation of transitional flows with laminar kinetic energy." Engineering Mechanics 20.5 (2013): 379-388.

50. Savill, A. M. "The effect of an adverse pressure gradient on the drag reduction performance of manipulators." International journal of heat and fluid flow 10.2 (1989): 118-124.

51. White, A. "Some observations on the flow characteristics of certain dilute macromolecular solutions." Viscous Drag Reduction: Proceedings of the Symposium on Viscous Drag Reduction held at the LTV Research Center, Dallas, Texas, September 24 and 25, 1968. Boston, MA: Springer US, 1969.

52. Lee, H., and S-H. Kang. "Flow characteristics of transitional boundary layers on an airfoil in wakes." J. Fluids Eng. 122.3 (2000): 522-532.

53. Puttkammer, P. P. (2013) Boundary layer over a flat plate. BS thesis. University of Twente.

54. Lighthill, M. J., and L. Rosenhead (1963) "Laminar boundary layers." Oxford University Press, USA: 5-88.

55. Morton, Bruce R. (1984) "The generation and decay of vorticity." Geophysical & Astrophysical Fluid Dynamics 28.3-4: 277-308.

56. SLOAN, DM. "Cottet, G.-H. and Koumoutsakos, PD (2001) Vortex methods: theory and practice (Cambridge, 2000), xiii+ 313 pp., 0 521 62186 0 (hardback),£ 37.50 (US $59.95)." Edinburgh Mathematical Society. Proceedings of the Edinburgh Mathematical Society 44.2 (2001): 445.

57. Dushane, Theodore E. (1973) "Convergence for a vortex method for solving Euler's equation." Mathematics of Computation 27.124 (1973): 719-728.

58. Hald, Ole H. (1979) "Convergence of vortex methods for Euler's equations. II." SIAM Journal on Numerical Analysis 16.5 (1979): 726-755.

59. Zhang, P. W. (1996) "Convergence of the point vortex methods for Euler equation on half plane." Journal of Computational Mathematics (1996): 213-222.

60. Chorin, Alexandre Joel. "Numerical study of slightly viscous flow." Journal of fluid mechanics 57.4 (1973): 785-796.

61. Barba, L. A., A. Leonard, and C. B. Allen (2004) "Advances in viscous vortex methods-meshless spatial adaption based on radial basis function interpolation." International Journal for Numerical Methods in Fluids, Int. J. Numer. Meth. Fluids 46 (2004): 001-0032.

62. Batchelor, George Keith. (2000) An introduction to fluid dynamics. Cambridge university press.

63. Carlton, J. (2012) "Marine Propellers and Propulsion, Third Edit." (2012). Ch. 7.

64. Xia, Xi, and Kamran Mohseni. (2017) "Unsteady aerodynamics and vortex-sheet formation of a two-dimensional airfoil." Journal of Fluid Mechanics 830 (2017): 439-478.

65. Hemati, Maziar S., Jeff D. Eldredge, and Jason L. Speyer (2014) "Improving vortex models via optimal control theory." Journal of Fluids and Structures 49 (2014): 91-111.

66. Du, Yiqing, and George Em Karniadakis. "Suppressing wall turbulence by means of a transverse traveling wave." Science 288.5469 (2000): 1230-1234.

67. Cousteix, T. Cebeci J., and J. Cebeci (2005) "Modeling and computation of boundary-layer flows." Berlin, Germany: Springer.

68. Roberts, L. S., Correia, J., Finnis, M. V., & Knowles, K. (2014). Investigation of forcing boundary layer transition on a single-element inverted wing in ground effect. In International Vehicle Aerodynamics Conference (pp. 14-15).